Tribology Transactions

ISSN: (Print) (Online) Journal homepage: https://www.tandfonline.com/loi/utrb20

Surface Roughness Influence on Tribological Behaviour of HiPIMS DLC Coatings

Sharjeel Ahmed khan, João Oliveira, Fabio Ferreira, Nazanin Emami & Amilcar Ramalho

To cite this article: Sharjeel Ahmed khan, João Oliveira, Fabio Ferreira, Nazanin Emami & Amilcar Ramalho (2023): Surface Roughness Influence on Tribological Behaviour of HiPIMS DLC Coatings, Tribology Transactions, DOI: 10.1080/10402004.2023.2197472

To link to this article: https://doi.org/10.1080/10402004.2023.2197472

Accepted author version posted online: 17 Apr 2023.

Surface Roughness Influence on Tribological Behaviour of HiPIMS DLC Coatings

Sharjeel Ahmed khan [a,b,*], João Oliveira [a], Fabio Ferreira [a], Nazanin Emami [b], Amilcar Ramalho[a,†]

[a]Department of Mechanical Engineering, CEMMPRE, University of Coimbra, Rua Luis Reis Santos, 3030-788, Coimbra, Portugal

[b]Department of Engineering Sciences and Mathematics, Division of Machine Elements, Luleå University of Technology, 97187 Luleå, Sweden

*__Correspondence:__ sharjeel.ahmed.khan@ltu.se;

[†]**Amilcar Ramalho** amilcar.ramalho@dem.uc.pt

ABSTRACT

The application of DLC coatings in dry machining of difficult-to-machine materials has been gaining popularity due to high inertness, low coefficient of friction (COF) and high hardness of these coatings. Although, the effect of surface roughness on the tribological properties of DLC coatings is of paramount importance, usually it is overlooked; and coatings performance analysis were accomplished generally on highly polished substrate. The generation of polished surfaces is time-consuming, labour-intensive process and, in most cases, not feasible for the industry due to its high cost. This article focuses on determining the effect of substrate (WC-Co) surface roughness on the load bearing capacity and tribological properties of DLC coatings deposited by High Power Impulse Magnetron Sputtering (HiPIMS) in Ne-Ar gas plasma. The DLC films were deposited onto WC-Co substrates with three different surface roughness profiles and their tribological performance were evaluated by a reciprocating tribotest. The high surface roughness resulted in increased wear rate due to high level of asperities and

liable to premature delamination of the coatings meanwhile causing severe damage to the counter body due to inhibition of transfer film formation.

KEYWORDS Coefficient of friction, Wear, WC-Co substrate, surface roughness, HiPIMS, DLC coating.

INTRODUCTION

Diamond like carbon (DLC) coatings are used in various high wear resistance applications like stamping, moulding, machining tools, dies and automotive industry due to their high chemical inertness, high hardness and low COF (1–4). The high wear resistance and hardness is endowed from the formation of sp^3 hybridized carbon atoms yielding high internal residual stresses that being beneficical in providing good mechanical properties, subsequently lead to poor adhesion of the coatings with the substrate (5). In order to mitigate poor adhesion, high residual stresses, compostional mismatch and variation in thermal expansion coefficient, application of interlayers like Cr, Si, Ti, Nb, Zr, W and gradient layers of SiC, TiN, TiC ,TiCN and CrN are commonly employed (6). Moreover, surface treatments processes like plasma nitriding of substrate have shown significant improvement in the coating adhesion, mechanical and tribological properties of DLC coatings (7, 8). Similarly, mechanical and tribological aspect of DLC coatings are influenced by incorporation of metal dopants that increase the critical load bearing capacity of the DLC coatings by reducing the internal stresses in the coatings (9). Nevertheless, the adhesion of the undoped or doped DLC coatings are significantly influenced by initial surface roughness of the substrate which is most often disregarded in tooling industries. The surface roughness quality of the substrate has a significant influence on the tribological performance of the coated surfaces. Due to its multiscale characters, roughness can vary at macro, micro and nanoscopic scale. Even a polished surface at macroscale contains

roughness/irregularities i.e., peaks, valleys and textures at micro, nano and atomic scale. Thus, the roughness should be in certain limit to ensure adequate adhesion of coatings and to realize their expected beneficial mechanical and tribological performance.

Previously researchers have analysed the effect of surface roughness on the tribological properties of different coatings deposited typically on steel-based substrates. Vicen et al. (10) studied the effect of surface roughness of C55 stainless steel substrate after deposition of WC/C coatings. The C55 steel substrate used for deposition had an average surface roughness *Ra* of 0.482, 0.072 and 0.039 µm. The authors reported that the poor surface finish (*Ra* = 0.482) depreciates the tribological performance and coatings deposition does not improve the tribological properties in comparison with uncoated substrate. Recently, Kolawole et al. (11) studied the effect of surface roughness on the tribological properties of hydrogenated DLC coatings deposited on tappet valve by Plasma Enhanced Chemical Vapor Deposition (PECVD) technique. The surface of tappet valve (AISI steel 52100) had an average surface roughness *Ra* of 0.3, 1 and 2 µm. It was reported that an optimal degree of surface smoothness is desirable for good adhesion of DLC coatings with the substrate, improved wear resistance and mechanical properties in automotive components. Similarly Cho et al. (12) studied the influence of surface roughness and DLC coatings on piston skirts from diesel engine using engine oil in boundary lubrication. Vladimirov et al. (13) studied the effect of surface roughness of substrate on DLC coating deposited on two different steel types i.e. R6M5 and 20Cr13. The authors concluded that surface roughness was a critical factor controlling the wear resistance of DLC coatings and optimal *R*-value is dependent on the coatings thickness 'h'. The ratio *R/h* of ~0.2-0.3 was found optimal for good wear resitance and tribological characteristics. Recently, Ferreira et al. (14) studied the influence of DLC topography preapred by different surface finishing technique after

PVD deposition to evaluate the tribological performance in piston ring/cylinder liner. The wear of the piston rings and counterbody is considerably impacted by surface roughness of DLC coatings. Renan et al. (15) also studied topographical evolution influence after plasma nitriding on grey and nodular cast iron on the tribological properties of DLC coating.

However, the surface roughness effect on coatings tribological performance was usually studied for steel-based substrate. Only limited studies were performed regarding effect of substrate surface roughness for DLC coatings on other substrate e.g. Si_3N_4 substrate (16). It is equally important for cemented carbide substrates as surface roughness quality could significantly influence the adhesion and tribological performance of coatings in machining and cutting tools applications.

Cemented carbide (WC-Co) is a widely used material for various tools applications in machining, forming, drilling and mining operation due to its excellent mechanical and wear resistance characteristics (17). WC-Co tools are generally coated with different coatings systems like carbides, nitrides and oxides of transition metals i.e. TiN, TiAlN, CrAlN, WC, CrC, Al_2O_3 and often diamond based coatings to further improve the wear resistance and increase the lifetime of the tool (18). As large majority of WC-Co tools are coated in industries before employing them in their final application. Generally, the coating deposition was performed on poor surface quality due to high cost associated with surface polishing stage and strenous process of grinding hard WC-Co. The poor surface quality could results in reduced adhesion of the coatings and adversely effect the tribological properties. Therefore, a certain degree of surface preparation could be vital to reduce the high points of asperities in cutting tools else it corresponds to elevated contact pressure causing flaking, chipping and premature failure of the coatings.

In this study the effect of surface roughness of WC-Co substrate was analysed for DLC coatings deposited in Ne-Ar gas plasma using HiPIMS technique. The adhesion, wear and tribological performance of the DLC coating on three different surface roughness conditions were analysed. Before, the deposition of DLC coatings an interlayer of Cr+CrN was deposited on all the samples. Beside application of interlayers, there was still a high significance of initial substrate surface roughness on the load bearing capacity, COF and wear coefficient of the DLC coatings. Moreover, the influence of substrate surface roughness on the wear coefficient of counterbody was analysed and formation of transfer films was realized on the counter body.

EXPERIMENTAL

Materials

Figure 1a shows the SEM morphology of polished cemented carbide (WC-Co) substrate used for deposition of DLC coatings. The WC grains have an average grain size of 1 micron and hardness of 1622 ± 11 HV_2 evaluted by diagonals of indent from Vickers hardness tester (Figure 1b). Table 1 shows the compositional analysis of WC-Co substrate analysed by Wavelength Dispersive X-ray (WDX) analysis showing Co binder percentage of ~6%.

The WC-Co substrates used for deposition have a diameter of 29 mm and 10 mm height. Table 2 summarize the roughness parameters of substrate with different surface finish employed for coating depostions. The As-received (As-rec) sample has a high surface roughness and the wear marks are due to the machining operation during cutting. The Rough polished (R-pol) sample is prepared by grinding the sample with a successive increase in the SiC abrasive paper number upto 2500 mesh number. Whereas, the mirror polished (M-pol) surface was prepared

initially by successive grinding with increasing SiC abrasive paper number and later polished using a diamond paste of 1 micron size until mirror like finish is obtained. The surface roughness profile of the substrate were analyzed by 2D stylus profilometer with a tip radius of 2 µm, prior to the deposition of the coatings. In order to isolate the waviness and shape deviation in the roughness profiles, cut off wavelength filter was used, for measurement of 2D roughness parameters in accordance with EN ISO 4827 standard.

DLC Coatings Deposition

Prior to coating deposition, the WC-Co substrates with different surface roughness were cleaned with ethanol and acetone in an ultrasonic bath for 15-20 minutes each. Then, the samples were glued on the aluminium substrate holder with thermally conductive paste. The holder rotates at 23.5 rpm around the central axis in the chamber during the deposition process. Figure 2 shows the schematic of the experimental setup used for the deposition of DLC coatings. A high vacuum of 3×10^{-4} *Pa* is established using combination of turbomolecular and rotary backing pump. The distance from the target to substrate is kept around 80 mm for optimum deposition.

The DLC coatings were deposited by HiPIMS using previously optimised deposition parameters. The details about the deposition conditions can be found in previous works of authors (19, 20). Inside the HiPIMS deposition chamber, the substrate surface was cleaned by using an ion gun generating Ar^+ ion using ion gun voltage and current of 36 V and 20 A respectively. A substrate holder bias of -150 V was kept for 40 minutes in this process. The Ar^+ ion etching treatment facilitates in improving the film adhesion. A Cr/CrN interlayer was deposited prior to the DLC coatings. Firstly, a Cr interlayer of ~400 nm thickness was deposited using direct current magnetron sputtering power source (DCMS) in Ar plasma at a pressure of 0.8 *Pa* and with –80 V

of substrate bias. Then, a CrN gradient layer with ~400 nm was deposited by gradually introducing 33% of N_2 gas in the chamber under otherwise similar deposition parameters as in previous step. A pure graphite target with 99.5% purity was used in deep oscillating magnetron sputtering mode (DOMS), a variant of HiPIMS, using a power supply. The DLC films were deposited in 50% of Ne + 50% of Ar gas discharge while maintaining a deposition pressure of 0.8 *Pa* and applying -80 V of substrate bias. The deposited DLC coatings have thickness of 700 nm. The use of Ne gas plasma improves the ionization fraction of carbon and sp^3/sp^2 ratio in the DLC coatings (20).

Characterization and Tribological Testing

The load bearing capacity and adhesion of the coatings with the substrate was evaluated using the scratch tester fitted with Rockwell-C diamond indenter of 200 µm tip radius, by linearly increasing the load from 4N to 70N. The tests were performed at scratch speed of 10 mm/min and loading rate of 100 N/min. An optical microscope was used for analysing the coating failure and determination of the critical load (L_C).

The tribological analysis of the DLC coating deposited on the WC-Co substrate is performed by lab built reciprocating tribometer (21) under dry condition with a stroke length of 2 mm and applied force of 10 N using a 100Cr6 steel ball of 10 mm diameter as a counter-body. The reciprocating tribometer was in accordance with ASTM standard G 133-02. The eccentric shaft connected with the lathe machine generates reciprocating motion in sinusoidal form with a frequency of 10 Hz and records the coefficient of friction variation during the sliding motion for maximum travel distance of 400 m (100,000 cycles) and 600 m (150,000 cycles). The measurements were performed in a relative humidity of 44-50 %. Table 3 summarizes the parameters and testing conditions employed during the reciprocating tribo-test. Three tests were

performed under each condition. The morphological and compositional characterization of the DLC coatings and steel balls after the tribological test were performed by scanning electron microscope. Energy dispersive X-ray (EDX) analysis was performed to differentiate the elemental contrast of the transfer material on the counter-body and the end of scratch.

The wear track was evaluated by 3D white light interferometer and depth profile being used for the estimation of wear volume *V* and wear coefficient *k* being estimated by Archard's equation (1) (22).

$$k = \frac{V}{Nx} \qquad \left(\frac{mm^3}{N.m}\right) \qquad (1)$$

Here, *V* is the wear volume, *N* is the normal load and *x* is the sliding distance. Whereas the wear volume of the steel ball was determined by measuring the average of the two diameters *d* on the worn region by using the equation (2) below

$$V = \left(\frac{\pi h}{6}\right)\left[\frac{3d^2}{4} + h^2\right] \qquad (2)$$

Here, *h* is the height of the material removed from the ball and is determined by

$$h = r - \left[r^2 - \frac{d^2}{4}\right]^{\frac{1}{2}} \qquad (3)$$

In equation (3); *r* is radius of the ball and *d* is diameter of the wear scar

The mechanical properties like hardness and reduced Young's modulus of the coatings was measured for the DLC coatings for all samples by nanoindentation using a Berkovich diamond indenter by applying a maximum load of 10 mN. A total of 10 measurements were performed to obtain a mean value and indentation depth was kept around 10% of coating thickness.

RESULTS AND DISCUSSION

Surface Roughness of Substrate

Figure 3 shows the 2D surface roughness profile of the WC-Co surface prior to the deposition of DLC coatings. As-rec sample showed the highest variation in the surface roughness profile whereas, the lowest variation in the surface roughness profile was observed in the M-pol sample. For R-pol sample, surface finish quality lies in between the M-pol and As-rec sample. Table 2 show roughness parameters; *Ra* (arithmetic mean roughness), *Rz* (mean peak to valley depth) and *Rsk* (roughness skewness) of three different substrates. The *Ra* of As-rec sample is 0.260 µm, R-pol is 0.017 µm and M-pol is 0.008 µm respectively. There is approximately one order of magnitude difference in the Ra between different sample roughness's. The purpose of this analysis is to identify the surface roughness quality at which the tribological and adhesion properties of the deposited coatings are not affected significantly while retaining the intended functionality of the coating. This would facilitate in selecting the surface roughness to aid in saving energy and time spent during the surface preparation stage of hard WC-Co before the deposition of coatings for different applications.

Load Bearing Capacity

Figure 4 shows the optical microscopy analysis of scratch testing on DLC coated WC-Co substrate with different surface roughness. The indenter moves across the surface inscribing with increasing load from 4-70 N. As seen in the microscopic optical image, the As-Rec sample, with high surface roughness, undergoes a coating failure at an early stage in comparison with the M-pol and R-pol samples. For As-rec sample, the first coating cracking – L_{C1} occurs at ~14 N, with coating chipping – L_{C2} at ~25 N and coating delamination – L_{C3} initiated at 33 N with more exposure of the substrate with increasing applied load upto 70 N. The R-pol sample showed improved adhesion of the coating with the substrate with L_{C1}, L_{C2} and L_{C3} of 21, 34 and 52.5 N respectively. The rough samples (R-pol and As-rec) showed formation of debris across the

scratch length. However, there is no observation regarding the debris formation and coating delamination for the M-pol sample. The load bearing capacity of the M-pol sample is better in comparison with the As-rec and R-pol samples. The slight cracking – L_{C1} and smearing – L_{C2} of the coatings for M-pol sample occurs at ~32.5 N and 62 N respectively.

Figure 5 shows the end of the scratch test for all three samples examined under scanning electron microscopy, combined with EDX elemental mapping to confirm the exposure to the substrate in the scratch test. SEM morphology shows that M-pol sample exhibited minute damages to the coatings which is also confirmed from the low Cr and absence of W in elemental maps demonstrating to be well adherent with the substrate. As, the surface roughness of the substrate is increased, the indenter delaminates the DLC coatings, and the interlayer of Cr is exposed and even reached upto the substrate material as W is being detected as well. However, this effect is more pronounced on the substrate having high surface roughness (As-rec). Further, the chipping of the coating is also observed in the adjacent region to the propagation of the scratch showing poor adhesion of coatings with rough surface. The presence of O shows that as the top layer of DLC coatings is removed the Cr interlayer gets oxidized upon exposure. Minute presence of Ne was also detected during the EDX analysis which even is not comparable and is associated with the plasma gas used in the deposition of DLC coatings. Moreover, the presence of the interlayer supports in resisting the delamination of the top DLC coat, however, initial surface roughness quality determines the overall performance criteria, as seen in the case of surface with poor surface quality i.e. As-rec sample showing coating delamination and exposure to the substrate underneath.

Nanoindentation

Figure 6 shows the hardness and reduced modulus of DLC coatings measured by the nanoindentation using an applied load of 10mN. The average hardness and reduced modulus of DLC coatings measured on all samples was ~26.5 GPa and ~248 GPa. However, a large variation in standard deviation was observed for hardness and reduced modulus for the samples with increasing surface roughness e.g. As-rec sample. This could be associated due to indentation depth in the range of the surface roughness of the substrate and inadequate landing of the indenter in the valley or peak point of asperity of the highly rough surface causing fluctuations. The high dispersion in hardness results does not correspond to the variation in the hardness of coatings, as surface topography does not influence the mechanical properties of the DLC coatings (23). Similar high scatter in the load-depth curves and deviation in hardness values was reported earlier with the reduction in surface roughness quality (24).

Coefficient of Friction

Figure 7(a) illustrates the variation in COF of the DLC coated WC-Co samples with different surface roughness tested for 100,000 cycles. Steel (100Cr6) ball was used as counterbody for the reciprocating tribotest with a stroke length of 2 mm under an applied load of 10 N. As, the test starts the COF increases rapidly and then drops quickly, the running-in duration was completed within the first 1500 cycles for all the sample with a slight plateau formed in the R-pol sample (inset of Figure 7(a)). A significant influence of surface roughness was observed on the COF of DLC coated WC-Co substrate. For As-rec sample, no steady state COF was realized. The COF instead increases with the increase in number of cycles due to high roughness of the substrate and inhibition of the transfer layer formation on the counter body, that have contributed towards an increase in COF (as elaborated in Figure 11). The rapid decrease in CoF for M-pol and R-pol sample after the running-in period was due to phenomena of third body formation and stable

transfer layer on steel counterpart as explained in the later section. Whereas the formation of stable transfer layer was inhibited due to ploughing action of high asperities in the As-Rec sample. Furthermore, during the tribotest, sudden variation/striation in COF was observed for both R-pol and M-pol sample before a steady state COF was realized, this could be associated to the formation, removal and regeneration of the transfer material (26) and smoothening of roughness profiles. Figure 7(b) show the averaged COF of steady state for last 40,000 cycles of the different sample tested at 100K and 150K cycles. The averaged steady state COF for R-pol sample is ~0.11 which is lower compared with M-pol sample with value of ~0.15 for both the sliding conditions. The decrease in COF could be correlated in R-pol case to the wear debris being accumulated in the valley of the roughness texture in comparison with M-pol case. As the roughness skewness parameter (Rsk) for R-pol case was slightly negative that favours entrapment of the wear debris during the tribotest and would reduce COF compared with M-pol sample. Similarly, in literature, with a slight increase in surface roughness at higher applied loads caused lowering of the COF (25).

Wear Rate

The wear track analysis of the WC-Co substrate coated with DLC showed high wear resistance and surface seems highly polished as observed in SEM images and 3D white light interferometer. The wear scars shows that the surface roughness significantly influences the tribological properties and showed higher wear rate as the surface roughness quality deteriorate. The wear track for 100K cycles showed that M-pol and R-pol samples showed lower wear in comparison with the As-rec sample. The width of the wear scar in As-rec was ~1 mm which is approximately double of the width of the wear scar observed for R-pol and M-pol samples as seen in SEM morphology (Figure 8, left). 3D-profile analysis of the wear scar (Figure 8 middle)

and the 2D depth profile (Figure 8 right) extracted from the middle region of the wear scar shows that wear depth increases with the increase in the surface roughness of the WC-Co substrate.

Figure 9(a,b) shows the wear rate of the DLC coated disc and steel counter-body respectively after a tribo-test for 100K and 150K cycles. The wear rate for As-rec DLC coated disc was 4.73×10^{-7} mm^3/Nm calculated from 100K cycles test, whereas the wear rate of the R-pol and M-pol samples was 2.41×10^{-8} mm^3/Nm and 1.74×10^{-8} mm^3/Nm respectively for similar number of cycles. As, the number of cycles increased for R-pol and M-pol samples to 150K, the wear rate for M-pol remained almost same with a value of 1.66×10^{-8} mm^3/Nm and wear rate for R-pol showed a slight increase with value of 2.72×10^{-8} mm^3/Nm respectively. The wear rate of the disc was evaluated by taking the depth profile of the 3D white light profilometry images in the middle as shown in the Figure 9(c). It is evident that the wear rate of the DLC coated disc for As-rec DLC coated disc was one order of magnitude higher than the wear rate of R-pol and M-pol sample even after testing for 150K cycles.

Moreover, Figure 9(d) shows the optical images of the wear crater formed on the balls after 100K & 150K cycles after the tribo-test against samples of different surface roughness. The wear volume of the balls was estimated by using the ball diameter and sphericity of the ball using equation (1-3) and as explained in (27). The average of ball wear scar diameter of the As-rec (967 µm) samples is significantly higher than the wear diameter of R-pol (338 µm) and M-pol (307 µm) sample for 100K cycles. The estimated wear rate for As-Rec sample was 2.15×10^{-6} mm^3/Nm which is two order of magnitude higher than the steel ball sliding against R-pol ($2.95\times10^{-8}mm^3$/Nm) and M-pol ($2.08\times10^{-8}mm^3$/Nm) sample respectively under similar conditions. For 150K cycles, the average diameter of ball crater increases slightly for R-pol (363 µm) and M-pol (352 µm) substrate and the wear rate for steel ball against R-pol was 2.87×10^{-8}

mm^3/Nm and for M-pol it was $1.64\times10^{-8}mm^3$/Nm. The wear of the counterbody for R-pol and M-pol sample after 150K cycles was observed almost similar to the test perfomed at 100K cycles. This is associated with formation of stable transfer layer on the counterbody as explained in the later section.

Figure 10 shows the 2D profile of the ball after reciprocating tribological test performed on DLC coated substrate of different surface roughness using surface profilometer. The actual ball profile is also measured and illustrated in the figure for comparison purpose. For example, in order to demonstrate the high wear of the counter body observed due to the high surface roughness a comparison between the As-Rec and R-pol DLC coated WC substrate was demonstrated. It is evident from the surface roughness profile of the steel ball that R-pol sample even after 150K cycles demonstrated much lower wear to the ball in comparison with the 100K cycles against the substrate with higher surface roughness (As-rec sample). Surface roughness can significantly influence the wear of the material. Here, 2D profile of 100Cr6 balls used as a counter-body indicated that poor surface finish has high impact yielding a higher wear rate. These results are in accordance with the literature where an increase in the roughness of substrate caused a higher wear of the counter-body material (28).

Compositional Analysis of Counterbody

Figure 11 shows the composition and elemental map analysis of counter-body tested against the DLC coated As-rec and R-pol samples after 100K and 150K cycles respectively. The presence of C, Fe and O confirms the presence and formation of transfer layer onto the steel ball. We can infer from the morphology of wear region of the ball that, R-pol samples forms a tribo-layer on the ball. Whereas, for As-rec sample, transfer layer was formed but due to the high roughness and asperities continuous removal of the tribo-layer occurred, that, superposed with the complete

removal of the coating, resulting in higher COF and wear. Moreover, the C element observed in the As-rec sample has been agglomerated into particles, whereas C presence is more uniform around the periphery of the wear region for R-pol sample and from the presence of Ar in the R-pol samples, we can deduce that the transfer layer remained intact and was a contributing factor towards lowering of COF and wear rate.

Wear Mechanism

The remarkable low friction and wear behaviour of DLC coatings stems from the formation of transfer layer on countersurface in a tribological process (29) . Figure 12 show the schematic of formation kinematics of third-body transfer layer on steel countersurface and influence of the surface roughness in retention of the transfer layer over steel counterpart. The formation of third-body is initiated by the formation of iron and DLC debris which undergoes oxidation in humid ambient air environment. Later, these particles coalescence into short platelets covering the surface of the counterbody. The transfer film primarily consists of the platelets composed of iron oxide and graphite particle. These particles are generated during a tribological process, including a mechanical mixing action with an important role of friction induced stresses. The formation of transfer film in DLC tribopair is accustomed to the presence of humid, oxygen rich environment, and it was stated that tribological performance of DLC coatings in vacuum environment is entirely different considering the inability to form oxides. (30).

In this work, stable transfer film was formed on surface with good surface finish (M-pol and R-pol) in comparison with poor surface finish (As-Rec). The delamination of the transfer layer from the countersurface of steel ball in As-Rec sample was triggered by the peak points of the asperities. The asperities in high roughness generate pressure spikes causing delamination of the DLC coatings exposing the carbide substrate and also inhibit the formation of stable transfer

layer on counterbody that dramatically increases the friction and wear rate (23). Although high surface roughness resulted in facile generation of large amount of iron and DLC wear debris however, ploughing action of asperities inhibits in stabilization of transfer layer and any formed transfer layer chip off easily and its role would be less dominant. However, once a stable and highly performant third body transfer film was formed over the counterbody in M-pol and R-pol sample, the wear rate remained unaffected and stable low wear and friction was observed even for higher travel distance (150K cycles).

While observing the wear track of M-pol sample, the excellent surface finish and non-adhesive nature of DLC coatings, restrict any accumulation of the wear debris in the track and they basically coalescence to form small platelets. Whereas, in R-pol sample showing slightly textured surface, wear debris were trapped in the valleys during the friction test at different sites of the wear tracks which could reduce friction compared with M-pol sample for the tested conditions. However, further studies could be performed in order to understand the wear behaviour of DLC coatings for M-pol and R-pol sample, over extended testing duration.

CONCLUSIONS

The effect of substrate (WC-Co) surface roughness on the tribological and load bearing capacity of the DLC coating were studied. It can be concluded that

- Surface roughness has a significant influence on the adhesion, COF and wear rate of the DLC coating. With increasing surface smoothness, the load bearing capacity of the DLC coatings improved significantly.
- The wear rate of DLC coatings and counterbody increases rapidly with the increase in surface roughness.

- The poor surface quality in As-rec sample restricts the formation or retention of uniform transfer layer on the steel counterbody that caused higher COF and wear rate.
- For good tribological and adhesion performance of the coatings, adequate surface preparation is indispensable for realizing the expected tribological performance of DLC coatings. i.e., preferably to M-pol or at least R-pol substrate.
- Further studies on influence of surface roughness of cemented carbide substrate on tribological properties of DLC coatings could be carried out in lubricating environment using commercial coolant employed in cutting and forming tools industry.

ACKNOWLEDGEMENT

The authors acknowledge Sandvik Coromant AB, Sweden for providing the cemented carbide (WC-Co) substrate for this work. We also thank Alireza Vahidi for assistance in deposition of DLC coatings. The authors would like to thank Dr. Todor Vuchkov at Instituto Pedro Nunes (IPN) for help with white light interferometry. The project has received funding from the European Union's Horizon 2020 research and innovation programme under the Marie Skłodowska-Curie grant agreement No. 860246. This research was sponsored by national funds through FCT – Fundação para a Ciência e a Tecnologia, under the project UIDB/00285/2020 and LA/P/0112/2020.

CONFLICT OF INTEREST

The authors report there are no competing interests to declare.

REFERENCES

(1) Banerji, A., Bhowmick, S., and Alpas, A. T. (2014) "High Temperature Tribological Behavior of W Containing Diamond-like Carbon (DLC) Coating against Titanium

Alloys," *Surf. Coatings Technol.* 241, pp. 93–104.

(2) Folea, M., Roman, A., and Lupulescu, N. B. (2010) "An Overview of DLC Coatings on Cutting Tools Performance," *Acad. J. Manuf. Eng.* 8, pp. 30–36.

(3) Choleridis, A., Sao-Joao, S., Ben-Mohamed, J., Chern, D., Barnier, V., Kermouche, G., Heau, C., Leroy, M. A., Fontaine, J., Descartes, S., Donnet, C., and Klöcker, H. (2018) "Experimental Study of Wear-Induced Delamination for DLC Coated Automotive Components," *Surf. Coatings Technol.* 352, pp. 549–560.

(4) Okubo, H., Kawada, S., Watanabe, S., and Sasaki, S. (2018) "Tribological Performance of Halogen-Free Ionic Liquids in Steel–Steel and DLC–DLC Contacts," *Tribol. Trans.* 61, pp. 71–79.

(5) Hao, T., Du, J., Su, G., Zhang, P., Sun, Y., and Zhang, J. (2020) "Mechanical and Cutting Performance of Cemented Carbide Tools with Cr/x/DLC Composite Coatings," *Int. J. Adv. Manuf. Technol.* 106, pp. 5241–5254.

(6) Yao, J., Yan, F., Chen, H., Chen, B., Yan, M., and Zhang, Y. (2022) "The Formation of Diamond-like Carbon Structure Anchored in the Nitrided Layer of M50 Steel during Plasma-Assisted Thermochemical Treatment," *Mater. Des.* 214, pp. 110378.

(7) Kovacı, H., Yetim, A. F., Baran, Ö., and Çelik, A. (2018) "Tribological Behavior of DLC Films and Duplex Ceramic Coatings under Different Sliding Conditions," *Ceram. Int.* 44, pp. 7151–7158.

(8) Dalibon, E. L., Charadia, R., Cabo, A., Trava-Airoldi, V., and Brühl, S. P. (2013) "Evaluation of the Mechanical Behaviour of a DLC Film on Plasma Nitrided AISI 420 with Different Surface Finishing," *Surf. Coatings Technol.* 235, pp. 735–740.

(9) Yetim, A. F., Kovacı, H., Kasapoğlu, A. E., Bozkurt, Y. B., and Çelik, A. (2021) "Influences of Ti, Al and V Metal Doping on the Structural, Mechanical and Tribological Properties of DLC Films," *Diam. Relat. Mater.* 120, .

(10) Vicen, M., Bokůvka, O., Nikolić, R. R., and Bronček, J. (2021) "Influence of the Surface Roughness of the C55 Steel on Its Tribological Properties after Application of the WC / C Coating," *Transp. Res. Procedia* 55, pp. 490–495.

(11) Kolawole, F. O., Kolawole, S. K., Varela, L. B., Kraszczuk, A., Ramirez, M. A., and Tschiptschin, A. P. (2021) "Effect of Substrate Surface Roughness on the Tribological Properties of Dlc-h Coatings on Tappet Valve," *Tribol. Ind.* 43, pp. 189–199.

(12) Cho, D.-H., Lee, S.-A., and Lee, Y.-Z. (2009) "The Effects of Surface Roughness and Coatings on the Tribological Behavior of the Surfaces of a Piston Skirt," *Tribol. Trans.* 53, pp. 137–144.

(13) Vladimirov, A. B., Trakhtenberg, I. S., Rubshtein, A. P., Plotnikov, S. A., Bakunin, O. M., Korshunov, L. G., and Kuzmina, E. V. (2000) "The Effect of Substrate and DLC Morphology on the Tribological Properties Coating," *Diam. Relat. Mater.* 9, pp. 838–842.

(14) Ferreira, R., Almeida, R., Carvalho, Ó., Sobral, L., Carvalho, S., and Silva, F. (2021) "Influence of a DLC Coating Topography in the Piston Ring/Cylinder Liner Tribological Performance," *J. Manuf. Process.* 66, pp. 483–493.

(15) Giacomelli, R. O., Salvaro, D. B., Bendo, T., Binder, C., Klein, A. N., and de Mello, J. D. B. (2017) "Topography Evolution and Friction Coefficient of Gray and Nodular Cast Irons with Duplex Plasma Nitrided + DLC Coating," *Surf. Coatings Technol.* 314, pp. 18–27.

(16) Shu, K., Zhang, C., Zheng, D., Gu, L., and Wang, L. (2020) "Delamination of Diamond-like Carbon Films on Rough Si 3 N 4 Surfaces," *Surf. Eng.* 36, pp. 770–779.

(17) García, J., Collado Ciprés, V., Blomqvist, A., and Kaplan, B. (2019) "Cemented Carbide Microstructures: A Review," *Int. J. Refract. Met. Hard Mater.* 80, pp. 40–68.

(18) Sousa, V. F. C., and Silva, F. J. G. (2020) "Recent Advances on Coated Milling Tool Technology—A Comprehensive Review," *Coatings* 10, pp. 235.

(19) Ferreira, F., Aijaz, A., Kubart, T., Cavaleiro, A., and Oliveira, J. (2018) "Hard and Dense Diamond like Carbon Coatings Deposited by Deep Oscillations Magnetron Sputtering," *Surf. Coatings Technol.* 336, pp. 92–98.

(20) Vahidi, A., Fonseca, D., Oliveira, J., Cavaleiro, A., Ramalho, A., and Ferreira, F. (2021) "Advanced Tribological Characterization of DLC Coatings Produced by Ne-HiPIMS for the Application on the Piston Rings of Internal Combustion Engines," *Appl. Sci.* 11, pp.

10498.

(21) Yasavol, N., and Ramalho, A. (2015) “Wear Properties of Friction Stir Processed AISI D2 Tool Steel,” *Tribol. Int.* 91, pp. 177–183.

(22) Archard, J. F. (1953) “Contact and Rubbing of Flat Surfaces,” *J. Appl. Phys.* 24, pp. 981–988.

(23) Soprano, P. B., Salvaro, D. B., Giacomelli, R. O., Binder, C., Klein, A. N., and de Mello, J. D. B. (2018) “Effect of Soft Substrate Topography on Tribological Behavior of Multifunctional DLC Coatings,” *J. Brazilian Soc. Mech. Sci. Eng.* 40, pp. 1–10.

(24) Chen, L., Ahadi, A., Zhou, J., and Ståhl, J.-E. (2013) “Modeling Effect of Surface Roughness on Nanoindentation Tests,” *Procedia CIRP* 8, pp. 334–339.

(25) Ravi, N., Markandeya, R., and Joshi, S. V. (2017) “Effect of Substrate Roughness on Adhesion and Tribological Properties of Nc-TiAlN/a-Si 3 N 4 Nanocomposite Coatings Deposited by Cathodic Arc PVD Process,” *Surf. Eng.* 33, pp. 7–19.

(26) Xu, P., Wang, Y., Cao, X., Nie, X., Yue, W., and Zhang, G. (2021) “The Tribological Properties of DLC/SiC and DLC/Si3N4 under Different Relative Humidity: The Transition from Abrasive Wear to Tribo-Chemical Reaction,” *Ceram. Int.* 47, pp. 3901–3910.

(27) Amanov, A., Pyun, Y. S., Kim, J. H., and Sasaki, S. (2014) “The Usability and Preliminary Effectiveness of Ultrasonic Nanocrystalline Surface Modification Technique on Surface Properties of Silicon Carbide,” *Appl. Surf. Sci.* 311, pp. 448–460.

(28) Ohana, T., Suzuki, M., Nakamura, T., Tanaka, A., and Koga, Y. (2004) “Tribological Properties of DLC Films Deposited on Steel Substrate with Various Surface Roughness,” *Diam. Relat. Mater.* 13, pp. 2211–2215.

(29) Härtwig, F., Lorenz, L., Makowski, S., Krause, M., Habenicht, C., and Lasagni, A. F. (2022) “Low-Friction of Ta-C Coatings Paired with Brass and Other Materials under Vacuum and Atmospheric Conditions,” *Materials (Basel).* 15, pp. 2534.

(30) Liu, Y., Chen, L., Zhang, B., Cao, Z., Shi, P., Peng, Y., Zhou, N., Zhang, J., and Qian, L.

(2019) “Key Role of Transfer Layer in Load Dependence of Friction on Hydrogenated Diamond-Like Carbon Films in Humid Air and Vacuum,” *Materials (Basel)*. 12, pp. 1550.

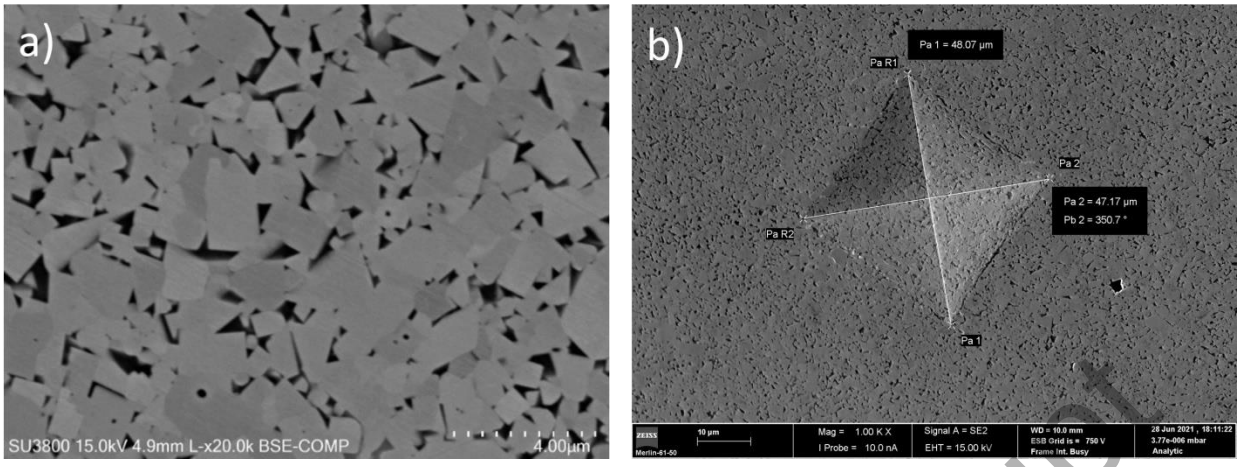

Figure 1: a) SEM morphology of polished WC-Co substrate and b) Vickers hardness indentation morphology showing hardness value of 1622±11 HV2

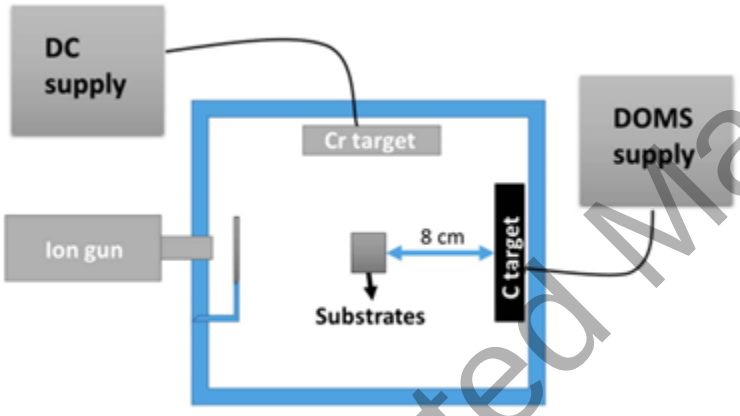

Figure 2: Schematic of coating deposition setup employed for the deposition of DLC coatings (14).

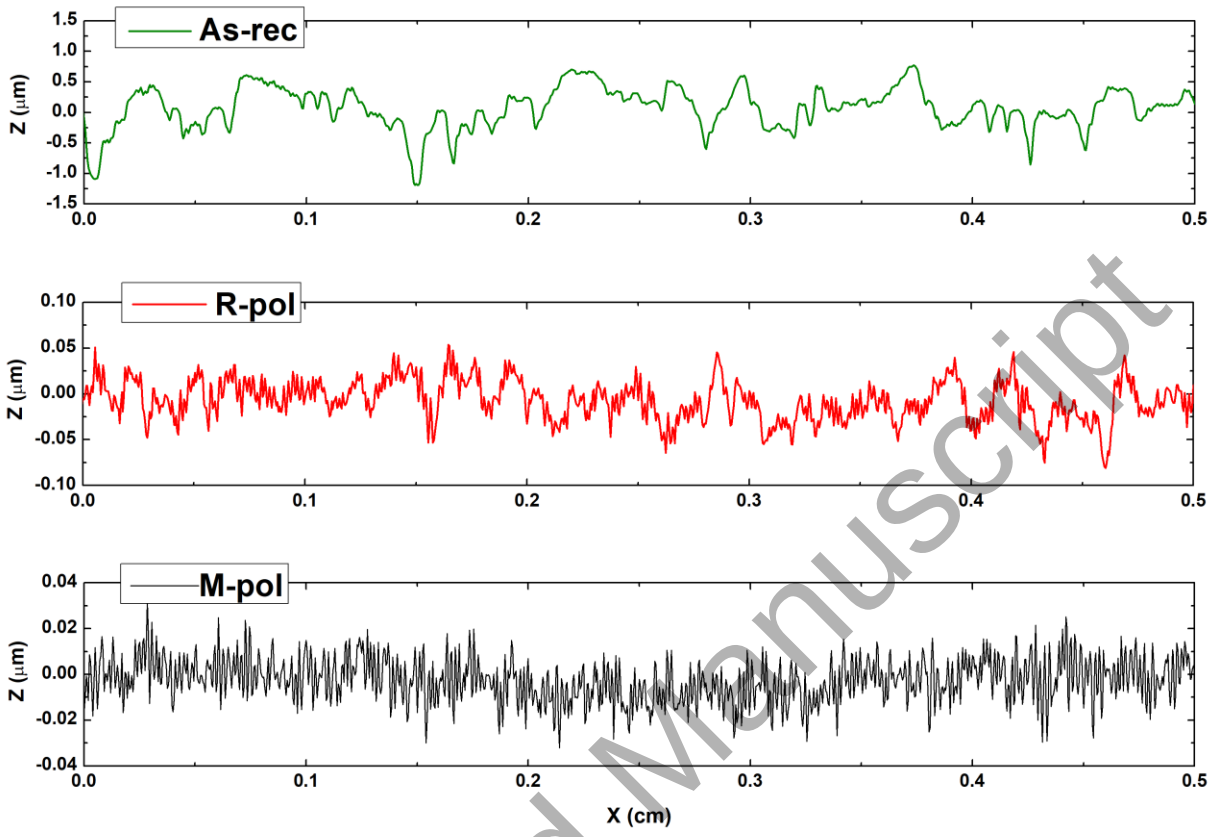

Figure 3: 2D surface Roughness profile of three different WC-Co samples measured for a distance of 0.5cm.

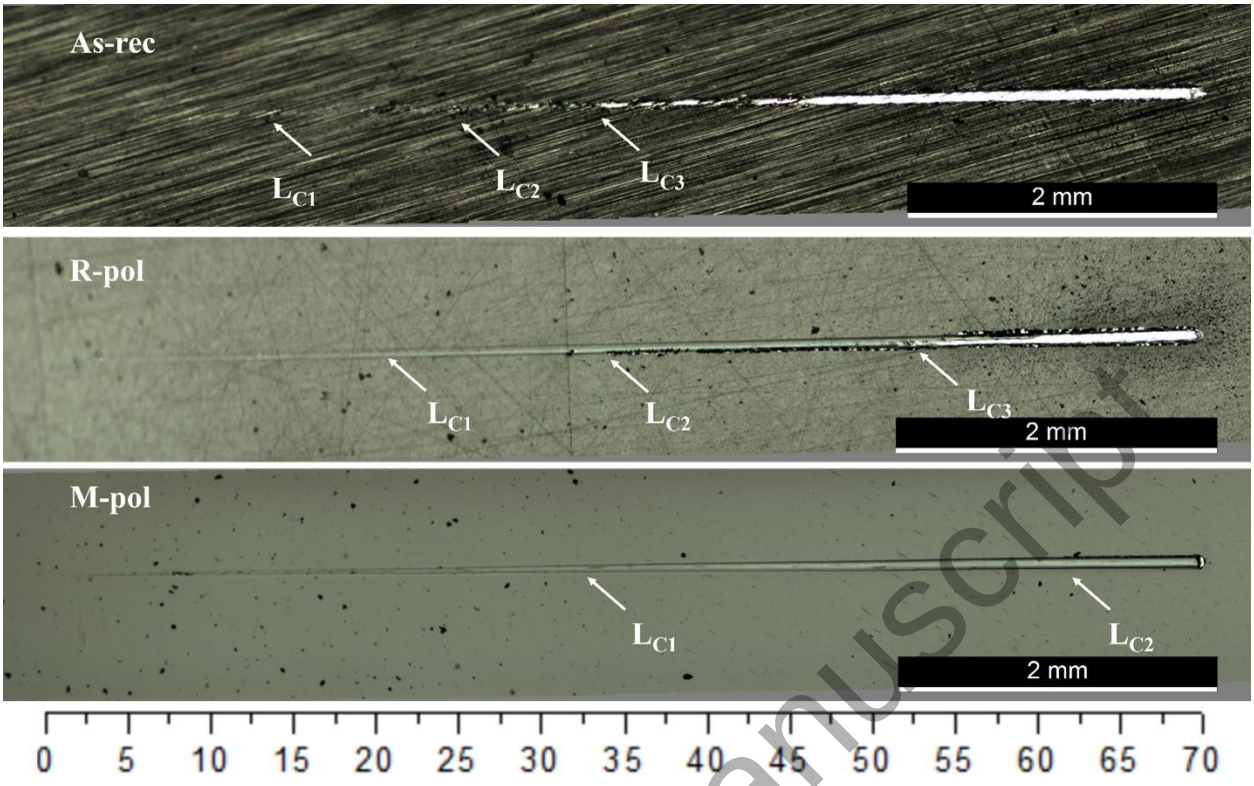

Figure 4: Scratch testing of the DLC coatings having different surface roughness of WC-10%Co substrate.

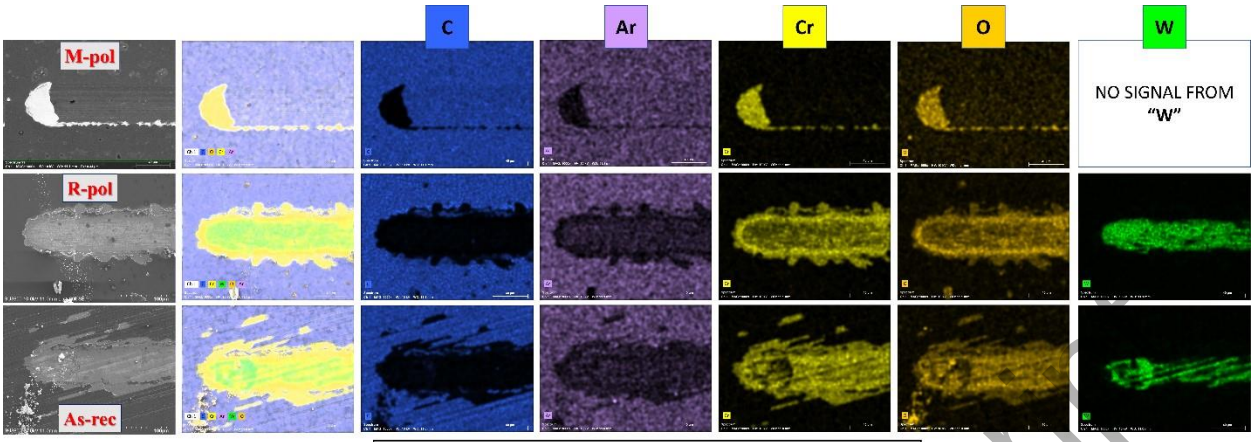

Element Percentage	M-pol	R-pol	As-rec
C	92.83	83.70	81.58
Ar	2.07	1.59	1.56
Cr	2.43	10.44	12.07
O	2.67	3.37	4.2
W	-	0.90	0.59

Figure 5: Elemental compositional map analysis of the end of the scratch for the DLC coated samples of varying substrate surface roughness. The table present the elemental atomic percentage for the mapped area.

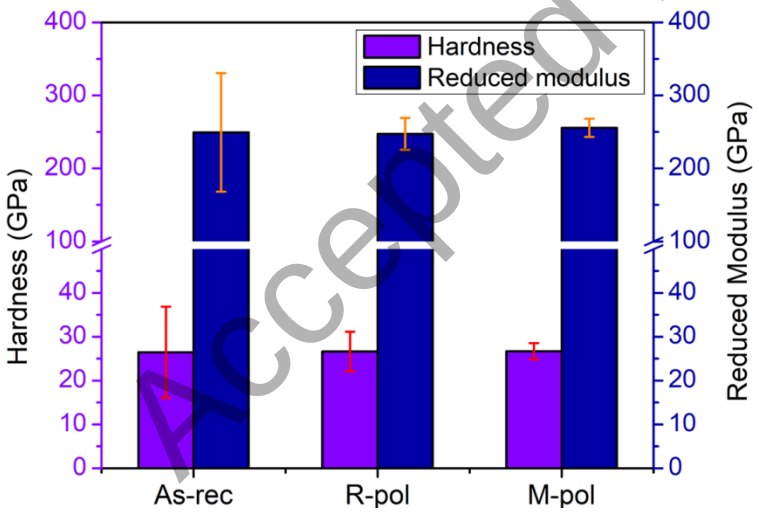

Figure 6: Hardness and Reduced modulus of the DLC coatings deposited on WC-Co substrate with different surface roughness.

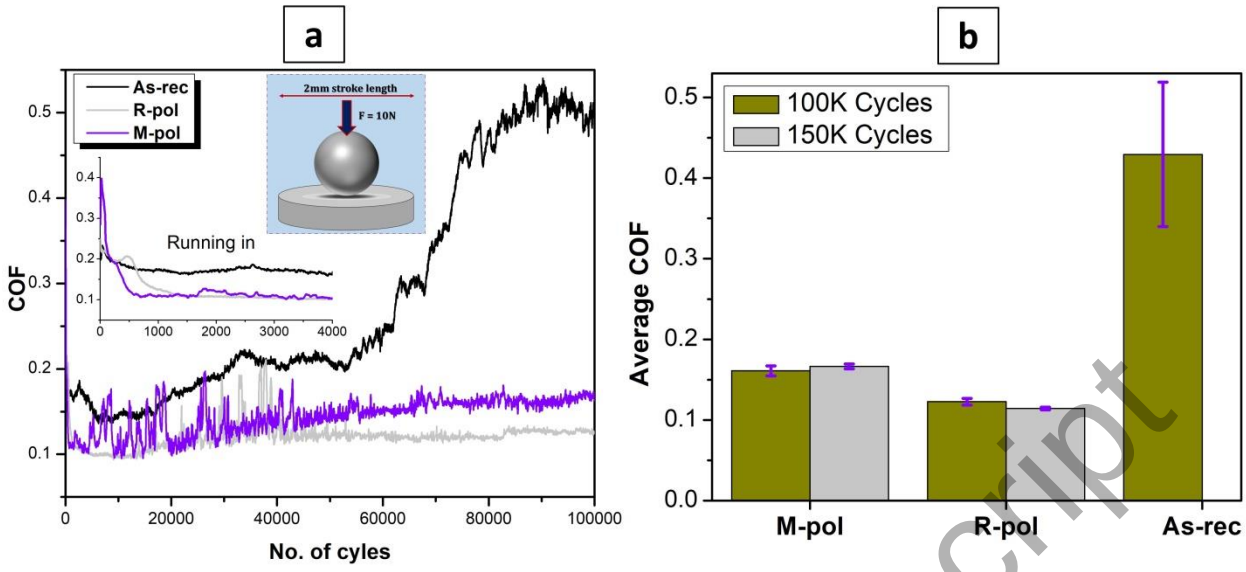

Figure 7: (a) COF analysis of the DLC coated samples with different surface roughness of WC-Co substrate. The inset shows details into the running-in period. (b) Average CoF for last 40000 cycles for substrate tested at 100K and 150K cycles.

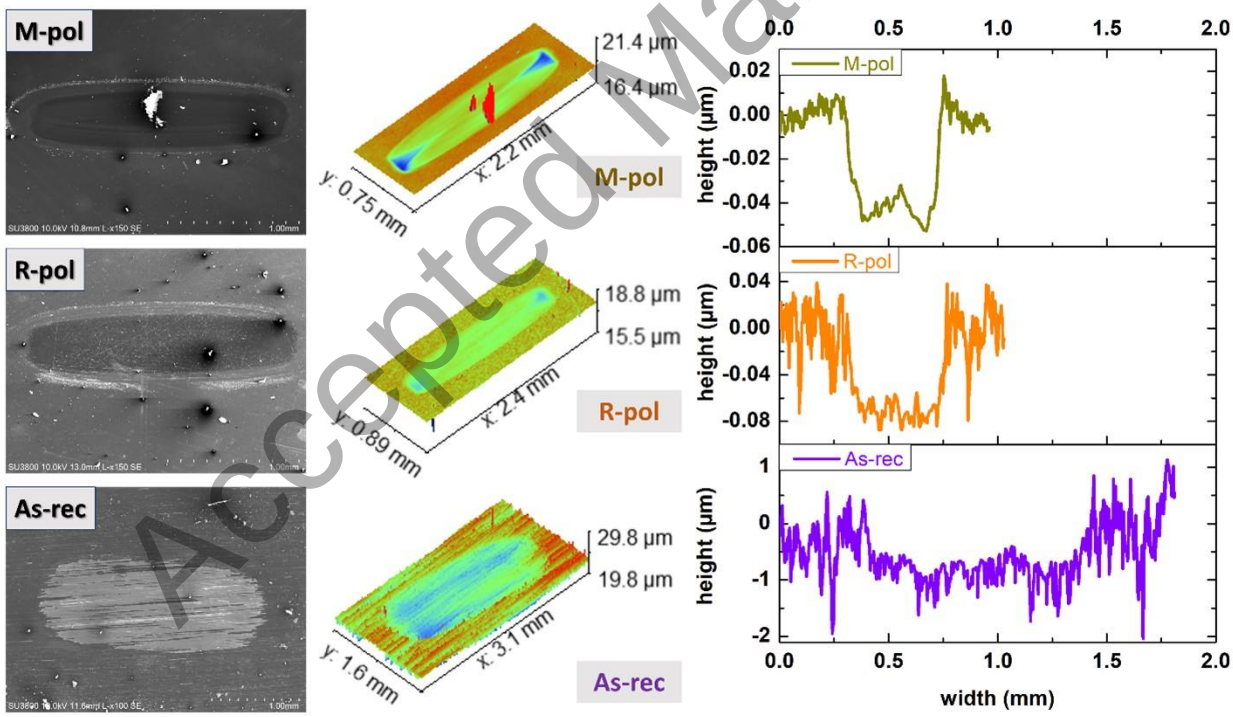

Figure 8: Morphological analysis, 3D topography and 2D depth profiles of the wear scar of DLC coated samples on different surface roughness after 100K cycle in reciprocating tribo-test.

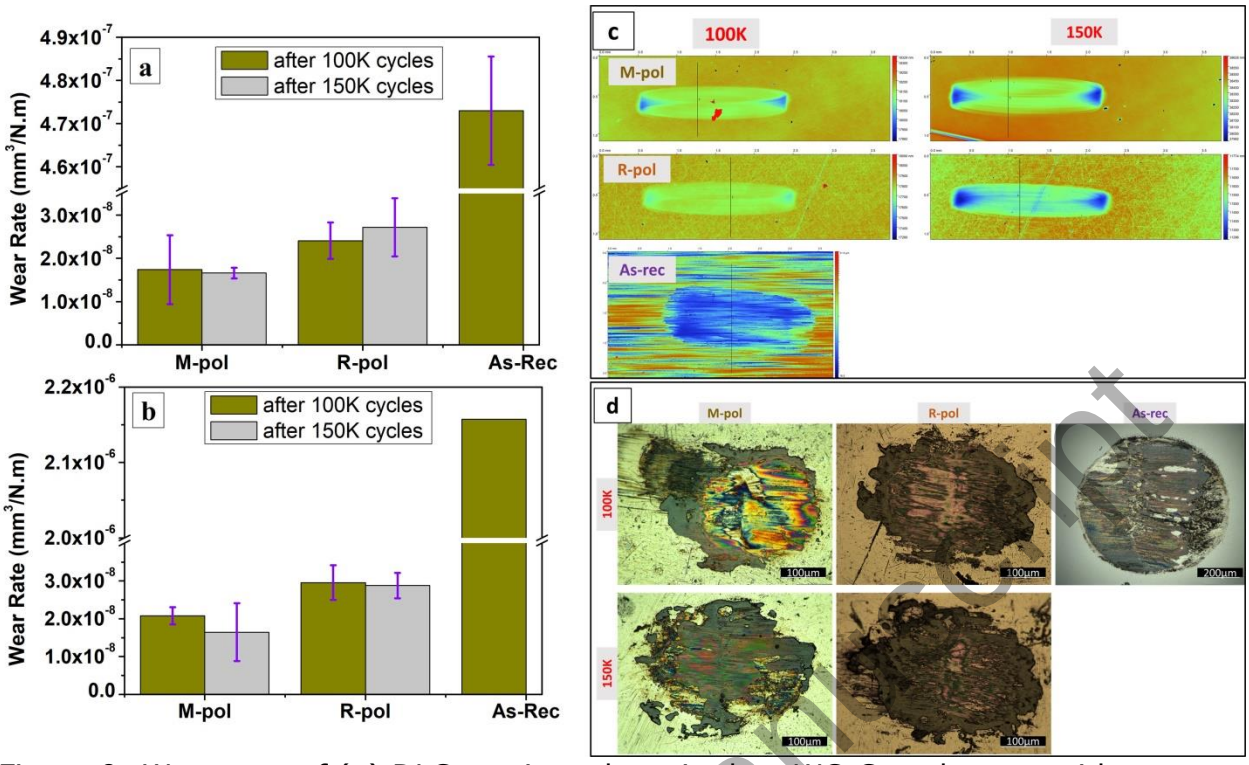

Figure 9: Wear rate of (a) DLC coatings deposited on WC-Co substrate with different roughness and measured from the (c) 3D profilometry of the worn region after reciprocating test. (b) Wear rate of counter-body after a tribo-test against different samples measured from average diameter of (d) Optical images of 100Cr6 ball. (Note: the scale of the counter-body slided against As-rec is 200 µm)

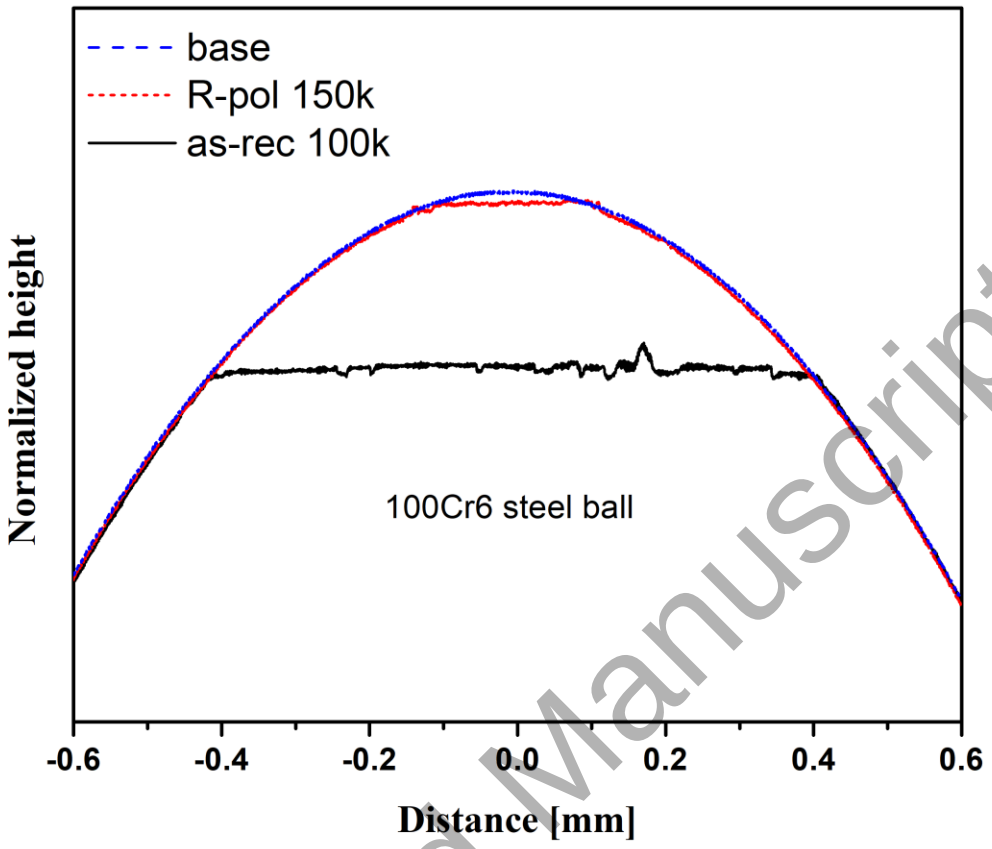

Figure 10: 2D wear profile of the 100Cr6 steel ball after reciprocating test against R-pol substrate for 150K cycles and as-rec coated substrate after 100K cycles.

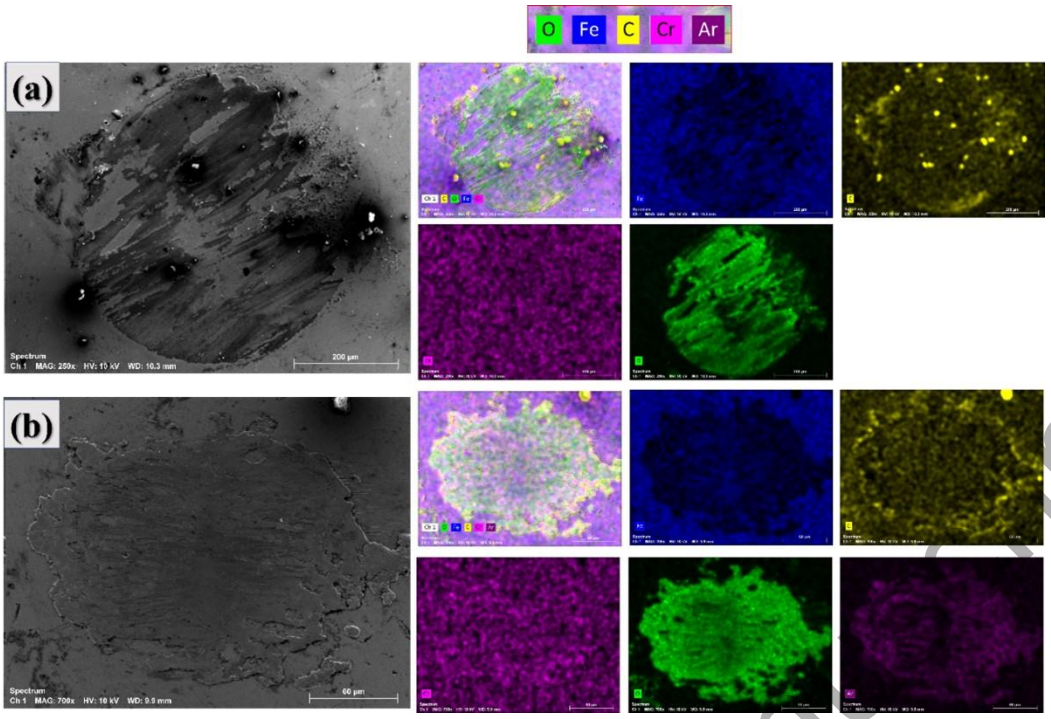

Figure 11: SEM morphology and elemental map of the wear of the steel ball following a reciprocating test against (a) As-rec sample after 100,000 cycles and (b) R-pol sample after 150,000 cycles. Note the scale of wear scar of both steel balls.

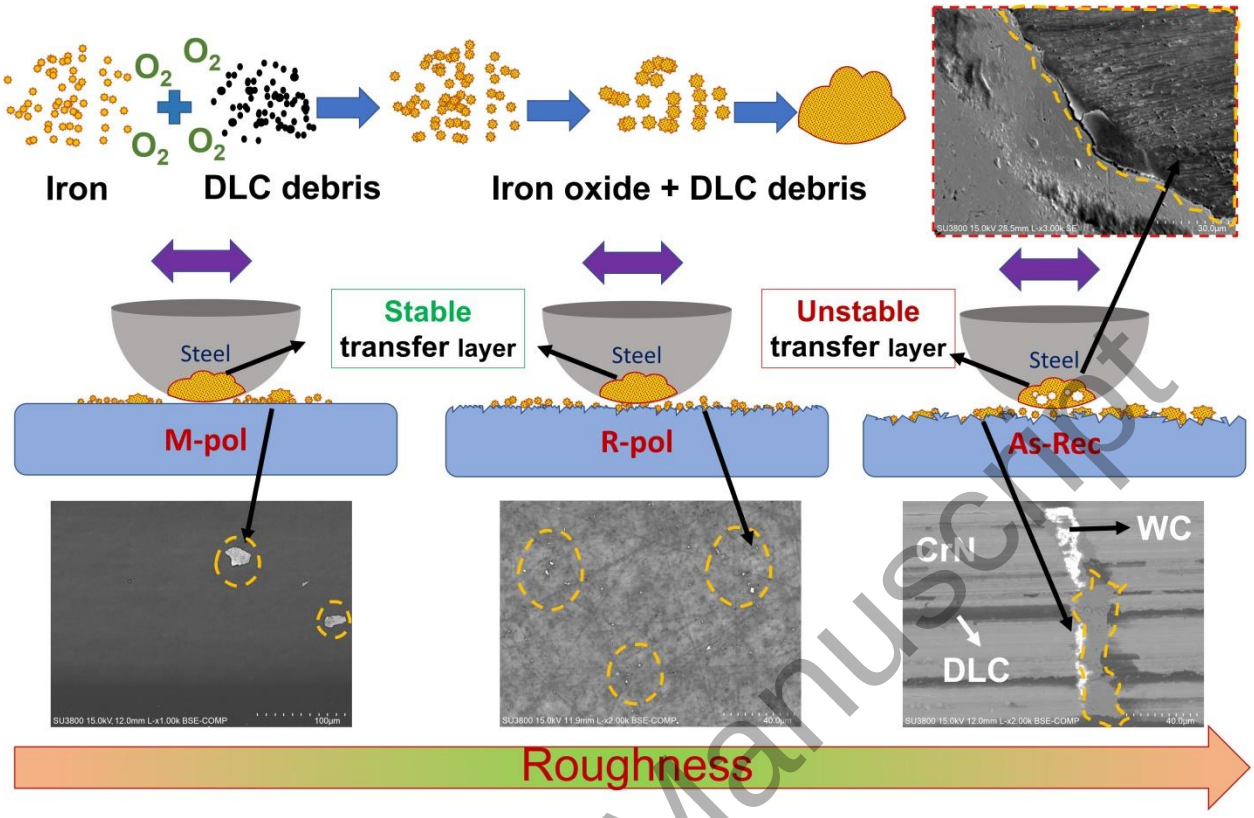

Figure 12: Schematic showing the formation of transfer layer on steel counterbody sliding against DLC coated WC substrate having different roughness.

Table 1: WDX analysis of WC-Co substrate

Element	Weight %
W	87.171
Co	5.827
C	7.097

Table 2: Visual inspection and roughness parameters (*Ra*) of the WC-Co substrate used for deposition

Samples	Abbreviation	Visual description	*Ra* (µm)	*Rz (µm)*	*Rsk*
As received	**As-rec**	The surface is dull and have visible textures and waviness.	0.260	1.14	-0.424
Rough polished	**R-pol**	The surface is not shiny, only minor scratches are observed	0.017	0.097	-0.181
Mirror polished	**M-pol**	Shinny and smooth with no visible marks (mirror like)	0.008	0.052	0.024

Table 3: Parameters and testing conditions during the reciprocating tribo-test.

Parameters	As-rec	R-pol	M-pol
No. of cycles	100K	100K, 150K	100K,150K
Relative humidity	46%	48-52 %	44%
Temperature	26 °C	24 °C	24 °C
Stroke length		2mm	
Frequency		10Hz	
Counter-body ball (Ø=10mm)		100Cr6 (820 HV_1)	
Normal load		10 N	
Lubricant		Dry	